

Rh(I) Complexes with Hemilabile Thioether-Functionalized NHC Ligands as Catalysts for [2 + 2 + 2] Cycloaddition of 1,5-Bisallenenes and Alkynes

Jordi Vila, Miquel Solà, Thierry Achard, Stéphane Bellemin-Laponnaz,* Anna Pla-Quintana, and Anna Roglans*



Cite This: *ACS Catal.* 2023, 13, 3201–3210



Read Online

ACCESS |

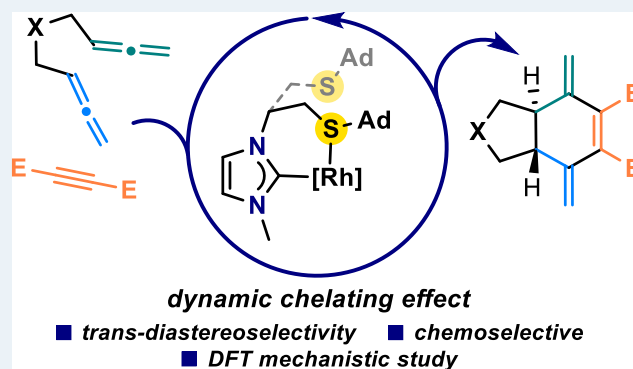
Metrics & More

Article Recommendations

Supporting Information

ABSTRACT: The [2 + 2 + 2] cycloaddition of 1,5-bisallenenes and alkynes under the catalysis of Rh(I) with hemilabile thioether-functionalized N-heterocyclic carbene ligands is described. This protocol effectively provides an entry to different *trans*-5,6-fused bicyclic systems with two exocyclic double bonds in the cyclohexene ring. The process is totally chemoselective with the two internal double bonds of the 1,5-bisallenenes being involved in the cycloaddition. The complete mechanism of this transformation as well as the preference for the *trans*-fusion over the *cis*-fusion has been rationalized by density functional theory calculations. The reaction follows a typical [2 + 2 + 2] cycloaddition mechanism. The oxidative addition takes place between the alkyne and one of the allenes and it is when the second allene is inserted into the rhodacyclopentene that the *trans*-fusion is generated. Remarkably, the hemilabile character of the sulfur atom in the N-heterocyclic carbene ligand modulates the electron density in key intermediates, facilitating the overall transformation.

KEYWORDS: [2 + 2 + 2] cycloaddition, allene, rhodium, N-heterocyclic carbene, DFT calculation



INTRODUCTION

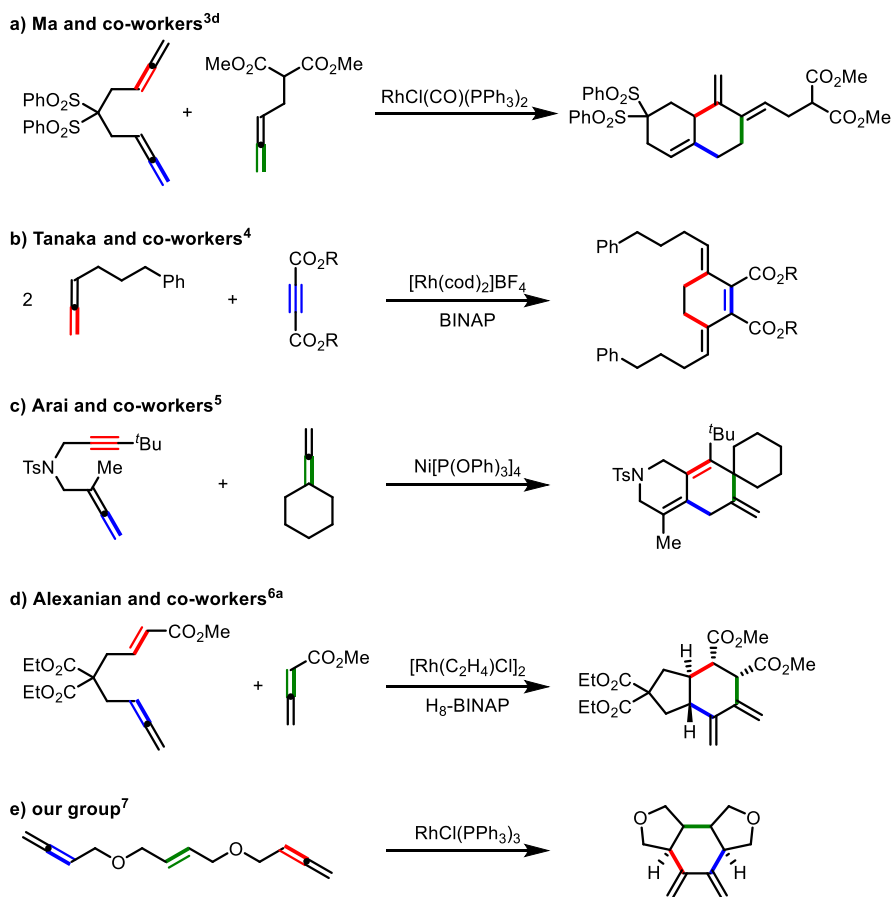
Transition-metal-catalyzed [2 + 2 + 2] cycloaddition reactions are a useful tool for the synthesis of six-membered carbo- and heterocyclic compounds in a one-step highly atom economic process.¹ The different types of unsaturation that can be involved in these processes open the door to a wide range of cyclic derivatives with different functionalities. Among the unsaturations that can be involved in the [2 + 2 + 2] cycloaddition reaction, allenes are particularly versatile as their two cumulated double bonds can individually participate in the cycloaddition. However, with this increased diversity comes greater difficulty in controlling chemoselectivity.² As the number of allenes involved in the [2 + 2 + 2] cycloaddition increases, the number of possible regioisomers also increases. After the pioneering studies by Benson and Lindsey^{3a} in 1958 based on the cyclotrimerization of allene by a Ni(0) catalyst, only a couple of studies by Ma and co-workers involve three allenes in a [2 + 2 + 2] cycloaddition to obtain steroid-like scaffolds.^{3b–d} Initially, the group described a bimolecular [2 + 2 + 2] cycloaddition of bisallenenes under rhodium catalysis giving a diene, which then underwent a Diels–Alder reaction with the remaining allene, giving precursors of steroidal structures.^{3b,c} A complementary approach to this process was the cycloaddition between a 1,5-bisallene and monoallenes

(Scheme 1a).^{3d} The reaction took place chemoselectively between an internal double bond and a terminal double bond of the bisallene and the terminal double bond of the monoallene under rhodium catalysis, giving a bicyclic derivative with two exocyclic double bonds. On the other hand, if we consider the participation of two allenes with an alkyne, we can find different processes based on the nature of the allenes and the nature of the transition metal used as the catalyst. Tanaka and co-workers⁴ described the cross-cyclotrimerization of two monosubstituted allenes with one alkyne to afford 3,6-dimethylenecyclohex-1-ene derivatives resulting from the cycloaddition of the terminal double bond of the allene (Scheme 1b). In contrast, when starting with di- or trisubstituted allenes and using the same catalytic system, a β -hydrogen elimination on the rhodacyclopentene intermediate took place instead of the insertion of the second allene,⁵ affording dendralene derivatives. Arai and co-workers⁶

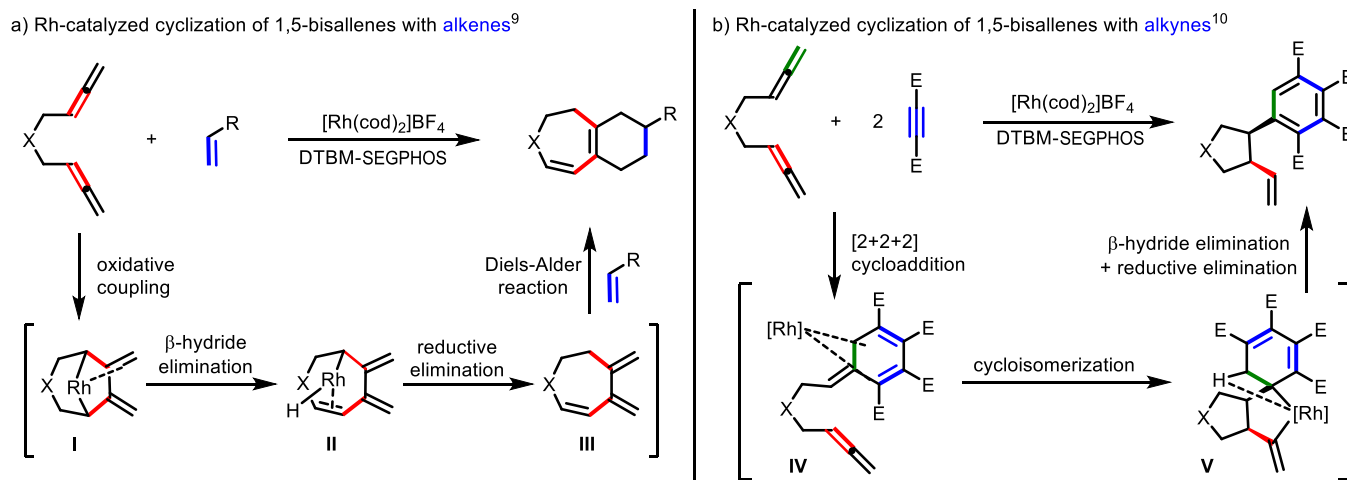
Received: November 25, 2022

Revised: January 12, 2023

Scheme 1. Metal-Catalyzed [2 + 2 + 2] Cycloaddition Reactions of Allenes

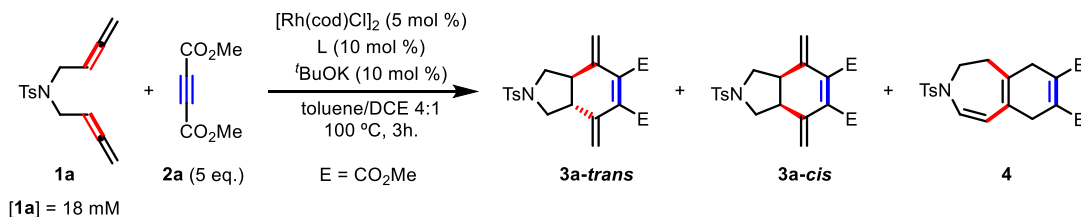


Scheme 2. Rh(I)-Catalyzed Cyclization Reactions of 1,5-Bisallenenes with Alkenes and Alkynes Performed in Our Group



reported the cycloaddition between two different allenenes and an alkyne under nickel catalysis and demonstrated by density functional theory (DFT) calculations that the selectivity of the reaction was affected by steric effects around the π -bonds (Scheme 1c). There are also examples involving an alkene with two allenenes that have been reported by both Alexanian and co-workers⁶ and our own group.⁷ Alexanian described the stereoselective and enantioselective rhodium-catalyzed [2 + 2 + 2] cycloaddition of ene-allenenes and allenates, affording *trans*-fused carbocycles with four stereogenic centers (Scheme 1d). The authors postulated an initial oxidative coupling of the

two allenenes involving the two internal double bonds of both allenenes. The alkene was then inserted into the rhodacyclopentane establishing the *trans* ring fusion in this step. We also studied the stereoselective cycloaddition of linear allene–ene–allene substrates to afford tricyclic systems.⁷ The Wilkinson complex promoted cycloaddition involving the internal double bonds of both terminal allenenes, affording the corresponding exocyclic dienes (Scheme 1e). DFT calculations showed that initial oxidative coupling took place between the internal double bond of one of the allenenes and the alkene, affording a *cis* ring fusion. The internal double bond of the second allene

Table 1. Optimization of the Rhodium(I)–NHC-Catalyzed [2 + 2 + 2] Cycloaddition of **1a** and **2a**

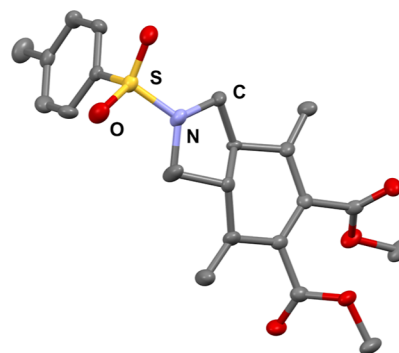
entry	ligand	variation of reaction conditions	yield (%) 3 (<i>trans</i> / <i>cis</i>)/ 4 ^a
1	L1		35 (83:17)/4
2	IPr-HCl		23 (78:22)/13
3	L2		51 (86:14)/10
4	L2	80 °C, 2 h	66 (86:14)/13
5	L3	80 °C, 2 h	61 (87:13)/10
6	L4	80 °C, 2 h	74 (89:11)/8
7	L5	80 °C, 2 h	61 (90:10)/7
8	L4	80 °C, 2 h, toluene	73 (93:7)/4
9	L4	80 °C, 2 h, toluene, [1a] = 36 mM	76 (93:7)/0
10	L4	80 °C, 2 h, toluene, 2a (2 equiv)	66 (91:9)/8
11	L4	80 °C, 2 h, toluene, 2a (10 equiv)	77 (92:8)/0
12	RhL4	80 °C, 2 h, toluene, RhL4 (1 mol %) [1a] = 36 mM	31 (91:9)/0
13	RhL4	80 °C, 2 h, toluene, RhL4 (2.5 mol %) [1a] = 36 mM	55 (91:9)/0
14	RhL4	80 °C, 2 h, toluene, RhL4 (5 mol %) [1a] = 36 mM	82 (92:8)/0
15	RhL4	80 °C, 2 h, toluene, RhL4 (10 mol %), [1a] = 36 mM	81 (92:8)/0

^aYields and ratios calculated by ¹H NMR from the reaction crude.

groups with different steric hindrances were attached to the sulfur atom in order to evaluate their influence in catalysis.

The stability of a complex formed with a bidentate ligand depends also on the size of the chelate rings. Our NHC-SR ligands L2-5 possess a flexible ethylene organic backbone, which can generate six-membered chelate rings. To evaluate this effect, the ligand L1 with a shorter N-arm was also prepared according to a literature procedure (Figure 1).^{22b}

Cycloaddition Catalysis. We started our study with the reaction of *N*-tosyl-tethered bisallene **1a** and dimethylacetylenedicarboxylate (DMAD) **2a** (Table 1). S-functionalized imidazolium salts L1-L5 (Figure 1) were tested as ligands. In the initial tests, the rhodium complexes were generated in situ by treatment of the corresponding imidazolium salt with ^tBuOK as a base and the dimeric rhodium complex [Rh(cod)Cl]₂. The reaction with L1 afforded three products, which were identified by NMR spectroscopy. In striking contrast to our previous studies with the same substrates (Scheme 2b),¹⁰ a mixture of diastereoisomers *trans* and *cis* **3a** in 35% yield with a ratio of about 5:1 was formed by a [2 + 2 + 2] cycloaddition reaction between the two internal double bonds of the two allenes of **1** and the alkyne (entry 1), also in contrast to the case of Ma (Scheme 1a) in which both an internal and an terminal double bond were involved in the reaction.^{3d} The molecular structure and stereochemistry of the major diastereoisomer **3a**, which was found to be *trans*, was confirmed by X-ray crystallographic analysis (Figure 2).³⁰ Of note, **3a** bears structural similarities to the product obtained through the intermolecular [2 + 2 + 2] reaction of two allenes and one alkyne described by Tanaka and co-workers (Scheme 1b).⁴ A second product **4** was also obtained, although with a very low yield. This was formed by our previously described process⁹ based on a cycloisomerization/Diels–Alder cascade reaction (see for instance Scheme 2a), in which in this case the dienophile is an alkyne (entry 1, Table 1). Interestingly, the

**Figure 2.** ORTEP representation of **3a-trans** at 50% of the probability level (CCDC 2209948).

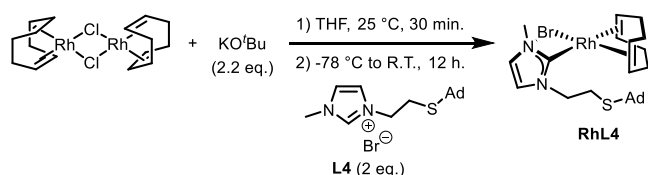
same reaction with the monodentate 1,3-bis(2,6-diisopropylphenyl)imidazolium chloride (IPr-HCl) provided lower selectivity and reactivity (entry 2, Table 1). In addition, the monodentate IMes and a bidentate OH-functionalized NHC or a bis-NHC have been less successful (see Scheme S2 in Supporting Information for details).

Encouraged by the selective formation of [2 + 2 + 2] cycloadducts **3** using this new catalytic system, we explored the other NHC-SR ligands and tested different reaction conditions to improve the efficiency and selectivity of the cycloaddition. Using imidazolium salt L2 with longer N-wing chain the yield of **3** improved to 51%, but the selectivity decreased (entry 3, Table 1). As a series of unidentified compounds were observed in the crude mixture in these experiments, the reaction was performed again by decreasing the temperature to 80 °C and the yield of **3** improved to 66% (entry 4, Table 1). Under these conditions, we proceeded to test the less sterically demanding NHC-SR ligands L3-5 (entries 5–7, Table 1). The use of ligand L4 provided the best yield and selectivity (entry 6, Table 1) and was thus selected for further tests. Performing the

reaction in the absence of DCE led to an increase in the *trans/cis* ratio and a decrease in the formation of **4** (entry 8, Table 1). To our delight, formation of byproduct **4** could be fully suppressed by increasing the concentration of **1a** from 18 to 36 mM (entry 9, Table 1). Increasing and decreasing the amount of **2a** (2 equiv and 10 equiv, respectively) did not improve the results (entries 10–11, Table 1). Once the ligand was optimized, we proceeded to prepare a preformed and well-defined Rh complex **RhL4**, which we used as a catalyst.

The NHC–rhodium(I) complex **RhL4** was prepared in a one-step process by the reaction of 2 equiv of imidazolium salt **L4** with 1 equiv of $[\text{Rh}(\text{cod})\text{Cl}]_2$ in the presence of 2.2 equiv of $t\text{BuOK}$ in THF (Scheme 3) following a procedure

Scheme 3. Synthesis of Rhodium Complex **RhL4**



previously described by us.³¹ The corresponding N-heterocyclic carbene complex **RhL4** was obtained in a high yield (above 95%) as a yellow shiny solid, which was fully characterized. In the presence of the halogen onto the metal center, no direct evidence of the coordination of the sulfur atom to the metal center was noticed by ^1H NMR.³²

The molecular structure of **RhL4** was confirmed by X-ray diffraction studies (Figure 3).³⁰ The rhodium–carbene bond

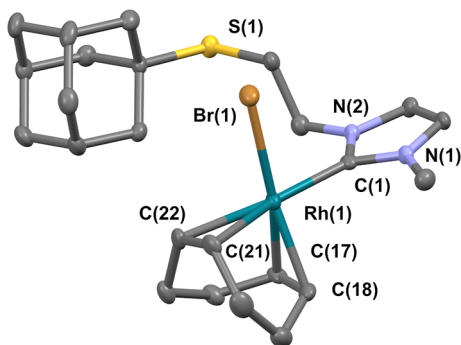


Figure 3. ORTEP representation of **RhL4** at 50% of the probability level (CCDC: 2213801). Selected bond lengths [Å] and angles [deg]: C(1)–Rh(1), 2.033(4); Rh(1)–Br(1), 2.5026(6); Rh(1)–C(17), 2.102(4); Rh(1)–C(18), 2.109(4); Rh(1)–C(21), 2.207(4); Rh(1)–C(22), 2.227(5); C(1)–Rh(1)–Br(1), 86.5(1); C(21)–Rh(1)–Br(1), 91.8(1); C(22)–Rh(1)–Br(1), 95.4(1); C(18)–Rh(1)–C(1), 94.2(2); C(17)–Rh(1)–C(1), 90.6(2).

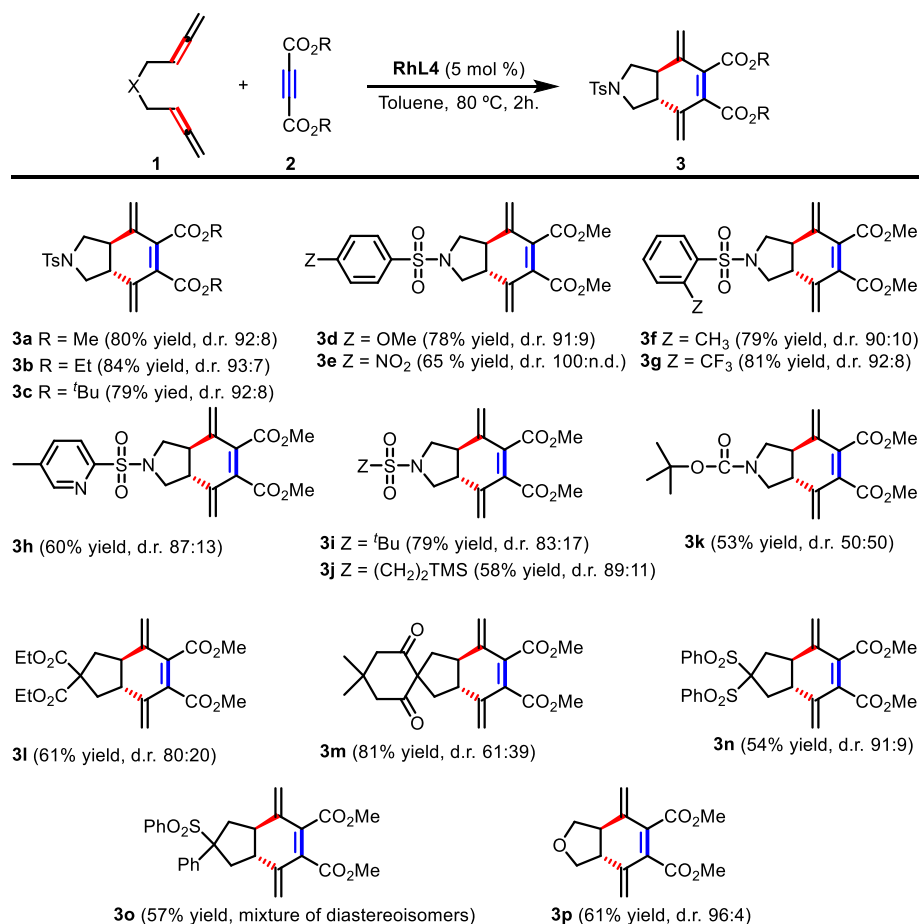
distance, 2.033(4) Å, is within the range reported for $[\text{RhCl}(\text{cod})(\text{imidazol-2-ylidene})]$ complexes.^{32,33} The Rh–C bonds located in a relative *trans* position to the carbene are significantly elongated (mean Rh–C 2.217 Å) compared to those in *trans* to the bromide ligand (mean Rh–C 2.1055 Å) due to the strong *trans* influence of the NHC ligand. The imidazole-2-ylidene ring is almost perpendicular to the coordination plane of the rhodium center (dihedral angle 88.64°), and this geometry is consistent with the ^1H NMR spectra.

Different catalytic amounts of **RhL4** were tested, from 1 to 10 mol % (entries 12–15, Table 1). Quantities below 5 mol % reduced the yield of **3a** (entries 12–13, Table 1) and the use of 10 mol % of **RhL4** (entry 15, Table 1) did not improve the results compared to the use of 5 mol % (entry 14, Table 1). It should be noted that in no case the formation of byproduct **4** was observed. Therefore, the optimal reaction conditions for further studies were defined as **1a** ($[\text{1a}] = 36$ mM), **2a** (5 equiv), **RhL4** (5 mol %) in toluene at 80 °C for 2 h (entry 14, Table 1). In addition, two blank tests were performed. The reaction was first carried out in the presence of the rhodium dimer $[\text{Rh}(\text{cod})\text{Cl}]_2$ excluding the NHC ligand and second in the absence of both the transition metal and the ligand. The reaction did not work in either case, and only the two starting products **1a** and **2a** were recovered.

It should be noted that bisphosphine ligands such as BINAP, Tol-BINAP, BIPHEP, DPEphos, Xantphos, and XPhos were not able to provide a defined product upon reaction of **1a** and **2a** as investigated in a previous study of our group.¹⁰

The scope of the reaction was then evaluated (Scheme 4). Methyl, ethyl, and *tert*-butyl acetylenedicarboxylates **2a**, **2b**, and **2c** were tested in the cycloaddition affording excellent yields and high *trans/cis* ratios³⁴ of the corresponding cycloadducts **3a**–**3c**. However, terminal alkynes, such as monoacetylenedicarboxylates and phenylacetylene analogues, did not react under these conditions. The nature of the substituents at the phenyl ring of the sulfonamide tether in bisallene **1** was then explored. The reaction proceeded efficiently with both electron-donating (**3d**) and electron-withdrawing groups (**3e**), as well as with substituents at the ortho position of the phenyl ring (**3f**, **3g**). A bisallene bearing the 5-methyl-2-pyridinesulfonyl group provided **3h** in a 60% yield, indicating that the presence of a potentially coordinating nitrogen atom did not poison the catalyst. Sulfonamide tethers with aliphatic substitution (*tert*-butyl and trimethylsilylethyl) were also efficient, delivering cycloadducts **3i** and **3j** in 79 and 58% yields, respectively. Changing the sulfonamide protecting group of the nitrogen tether to a carbamate (*N*-Boc bisallene), the reaction took place, although cycloadduct **3k** was obtained in a moderate yield and with low diastereoselectivity. Bisallenes with a carbonyl group attached to the quaternary carbon atom of the tether also participated in the cycloaddition, affording **3l** and **3m** with 61 and 81% yields, respectively. When the carbonyl group was substituted for arylsulfonyl groups, lower yields of the cycloadducts **3n** and **3o** were obtained, but the diastereoisomeric ratios were better. In the case of **3o**, an inseparable mixture of diastereoisomers was obtained due to the chiral center in the tether making it difficult to determine the diastereoisomeric ratio. Finally, oxygen-tethered bisallene participated in the process affording cycloadduct **3p** with a 61% yield and an excellent diastereoisomeric ratio.

Computational Analysis. Intrigued by the role of the hemilabile NHC-SR ligand in the chemoselectivity of the rhodium-catalyzed cycloaddition of 1,5-bisallenes and alkynes, we performed DFT calculations on the entire reaction. The Gibbs energy profile computed at 353.15 K and 1 atm with the $\omega\text{B97X-D/cc-pVTZ-PP/SMD}(\text{toluene})/\text{B3LYP-D3/cc-pVDZ-PP}$ method is depicted in Figure 4, and the molecular structures of all intermediates and transition states (TSs) are available in the Supporting Information (see Supporting Information for a complete description of the computational methods and Table S1 for a justification of the density functional employed).

Scheme 4. Scope of the [2 + 2 + 2] Cycloaddition Reaction of Bisallenes **1** and Alkynes **2**

The reaction starts with the coordination equilibrium of 1,5-bisallene and DMAD with the rhodium catalyst to give Rh(I) 16 e⁻ square planar complexes **A1** and **A1'** (Figure 4) (see Figure S1 for the whole set of coordination complexes). The coordination of the two internal double bonds of the 1,5-bisallene (**A1**) is the most exergonic process, releasing 6.6 kcal·mol⁻¹. For the upcoming oxidative cyclometallation, all possible orientations have been evaluated along with the dynamic chelating effect of the sulfur (see Figures S2 and S3), resulting in two possible TSs for each orientation: one with the sulfur chelating the rhodium (TSs superindexed with S in Figure 4) and the other without such a chelation.³⁵ Since **A1** and **A1'** (and the rest of the possible coordination complexes) are in equilibrium, according to the Curtin–Hammett principle,³⁶ the major rhodacyclopentene or rhodacyclopentane intermediate formed is the one generated through the lowest in energy TS, in this case TS^S(**A1'A2**). This TS involves an oxidative cyclometallation of the central carbon of one of the allenes of the 1,5-bisallene **1a** with DMAD **2a** with the sulfur chelating the rhodium. Formation of rhodacyclopentene intermediate **A2** takes place with an affordable barrier of 16.7 kcal·mol⁻¹ [**A1** to TS^S(**A1'A2**), being 7.6 kcal·mol⁻¹ lower than its non-chelating counterpart (TS(**A1'A2**), ΔG[‡] = 24.3 kcal·mol⁻¹]. This step **A1** ⇌ **A1'** → **A2** is exergonic by 31.6 kcal·mol⁻¹. Alternative ways to generate **A2** through other coordination complexes including **A1** have higher energy barriers (see Figures 4 and S2 and S3 in Supporting Information). For this path, the sulfur-assisted TS [TS^S(**A1'A2**)] is lower in energy than its analogue in which

the sulfur is not coordinated to the rhodium [TS(**A1'A2**)] due to the S electron-donating character, which adds electronic density to the rhodium and facilitates its oxidation [NPA charges on Rh are -0.101 e in TS(**A1'A2**) and -0.443 e in TS^S(**A1'A2**)]. However, in the oxidative cyclometallation from **A1**, coordination of S leads to a pyramidalization of the rest of the ligands coordinated to Rh. Pyramidalization brings the ligands closer to one another and, consequently, the two coordinated double bonds in the 1,5-bisallene become perpendicularly arranged to one another. This perpendicular arrangement is destabilizing³⁷ and the trend is inverted. As a result, the non-chelated TS(**A1A2**) is lower in energy than TS^S(**A1A2**) by 5.3 kcal·mol⁻¹. **A2** is a Rh(III) 18 e⁻ complex and exhibits an octahedral geometry in which the three carbons from the reacted allene are η³-coordinated to the rhodium (*d*_{Rh-C} = 2.217, 2.129, and 2.218 Å). This type of π-allyl metallacycle intermediates have previously been postulated in cycloaddition reactions.³⁸ From this point, **A2** needs to rearrange to set a coordination position free for the second allene unit, giving either **A3_{trans}** or **A3_{cis}** at the cost of 18.0 and 24.0 kcal·mol⁻¹, respectively. For the formation of the *trans*-fused rhodabicyclo intermediate **A4_{trans}** through **A3_{trans}**, the insertion (via the Schore mechanism³⁹) of the internal double bond of the second allene takes place in the Rh–C sp³ bond through TS^S(**A3A4**)_{trans}. This process **A2** → **A4_{trans}** has a total Gibbs energy barrier of 24.4 kcal·mol⁻¹ and is exergonic by 3.4 kcal·mol⁻¹. In contrast, for the formation of **A4_{cis}**, the insertion is found to occur in the Rh–C sp² bond, surpassing a Gibbs energy barrier of 27.0 kcal·mol⁻¹ [TS^S(**A3A4**)_{cis}] and releasing

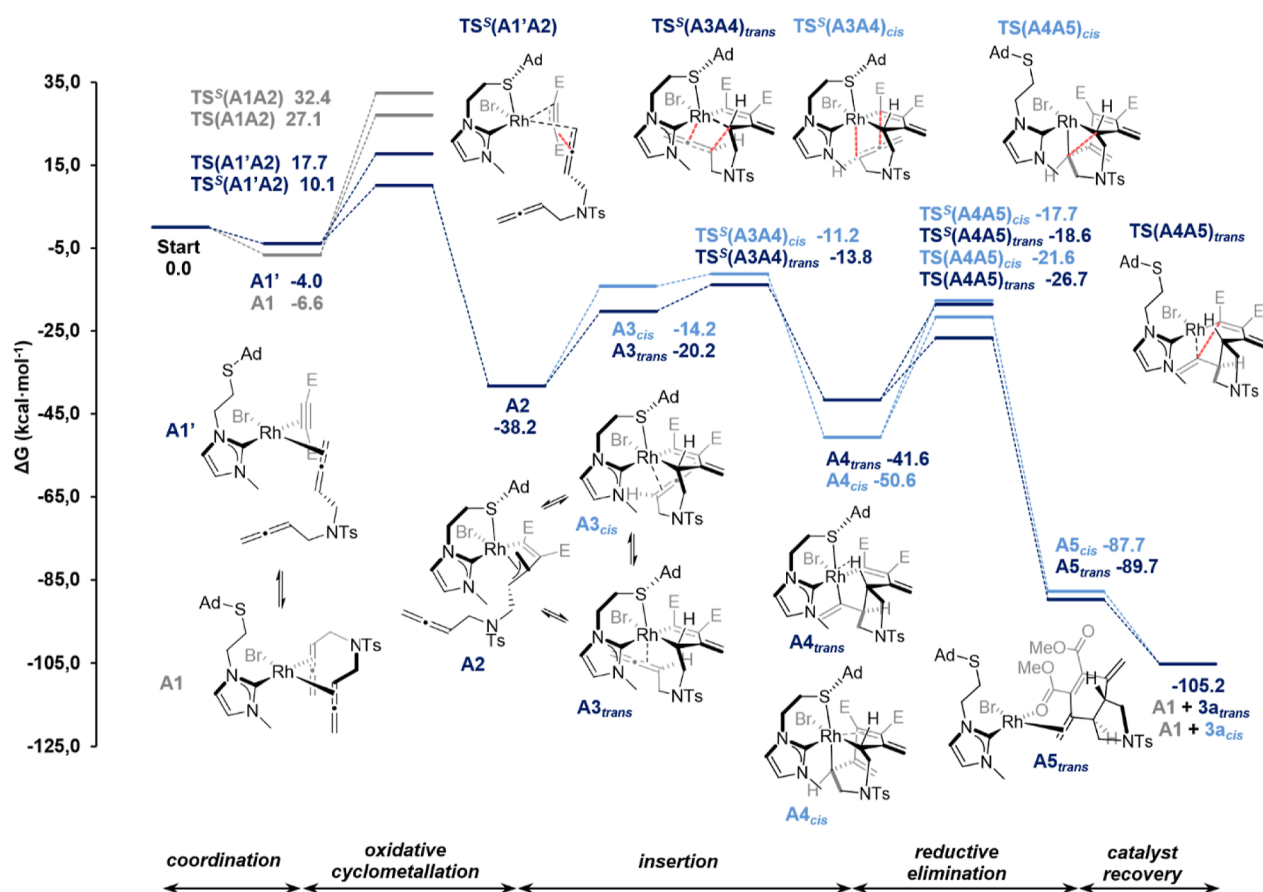


Figure 4. Gibbs energy profile (in kcal·mol⁻¹) for the cycloaddition of 1,5-bisallene **1a** and dimethylacetylenedicarboxylate **2a** leading to **3a** (E = CO₂Me).

12.4 kcal·mol⁻¹. The coordination of a second DMAD unit to **A2**, which would lead to our previously reported *cis*-3,4-arylvinyl pyrrolidine derivative (Scheme 2b),¹⁰ was also considered. However, it was found to be disfavored at the experimental concentration of DMAD (see Figure S6 in Supporting Information).

For the final reductive elimination step, the *S*-adamantyl functionality is dissociated from the rhodium center to remove electronic density, drastically reducing the Gibbs energy barriers by 8.1 kcal·mol⁻¹ [TS(A4A5)_{trans} vs TS^S(A4A5)_{trans}] and 3.9 kcal·mol⁻¹ [TS(A4A5)_{cis} vs TS^S(A4A5)_{cis}]. Finally, ligand exchange from **A5_{trans}** and **A5_{cis}** releases **3a-trans** and **3a-cis** and gives **A1** to restart the catalytic cycle. The formation of byproduct **4** (Table 1) was also evaluated computationally, and the results account for its formation in minor quantities at low concentrations of **2a** (see Scheme S6 and Figures S4 and S5 in Supporting Information for the complete discussion).

In summary, the reaction follows the typical [2 + 2 + 2] cycloaddition mechanism⁴⁰ and has an overall reaction energy of -98.6 kcal·mol⁻¹ ($\Delta G = G_{3a} - [G_{1a} + G_{2a}]$), almost identical for both diastereoisomers. For **3a-trans**, the energetic span between the turnover-frequency-determining intermediate (TDI, **A2**) and the turnover-frequency-determining TS (TDTS, TS(A3A4)_{trans}) is 24.4 kcal·mol⁻¹, and for **3a-cis**, the energetic span between TDI (**A4_{cis}**) and the TDTS [TS(A4A5)_{cis}] is 29.0 kcal·mol⁻¹.⁴¹ The allene–allene oxidative cyclometallation is found to be much higher in energy than the allene–alkyne oxidative cyclometallation ($\Delta\Delta G^\ddagger = 16.0$ kcal·mol⁻¹), indicating that the ring fusion stereochemistry comes

from the latter insertion^{6b} of the second allene, in which the insertion leading to the *trans* isomer [TS(A3A4)_{trans}] is preferred over the *cis* [TS(A3A4)_{cis}] by 2.6 kcal·mol⁻¹. This difference in energy is translated into a 98:2 *trans/cis* ratio using the Eyring equation, in perfect agreement with the experimental data.

In conclusion, the hemilability of NHC-SR ligands enabled an efficient rhodium-catalyzed [2 + 2 + 2] cycloaddition of 1,5-bisallenenes and alkynes. A number of N-, C-, and O-tethered 1,5-bisallenenes as well as variously substituted alkynes were successfully used in the reaction. The methodology developed gives access to bicyclic 3,6-dimethylenecyclohex-1-ene derivatives. Importantly, the exocyclic alkenes in the product scaffold provide ample opportunities of synthetic manipulation to build more complex molecules. A mechanistic investigation by means of DFT calculations has been carried out to unravel that a canonical [2 + 2 + 2] reaction manifold accounts for the observed transformation and that the hemilabile character of the sulfur in the ligand precisely modulates the electron density in key intermediates and facilitates the overall transformation. This hemilability in the catalytic system is expected to be useful for further development of demanding cycloaddition reactions.

■ ASSOCIATED CONTENT

Supporting Information

The Supporting Information is available free of charge at <https://pubs.acs.org/doi/10.1021/acscatal.2c05790>.

Experimental procedures, compound characterization data including NMR spectra for all new compounds, and computational data (PDF)

Crystallographic data of 3a (CIF)

Crystallographic data of RhL4 (CIF)

Crystallographic data of [RhL4][PF₆] (CIF)

AUTHOR INFORMATION

Corresponding Authors

Stéphane Bellemin-Lapponaz – Institut de Physique et Chimie des Matériaux de Strasbourg, CNRS-Université de Strasbourg, UMR7504, 67034 Strasbourg, France; orcid.org/0000-0001-9462-5703; Email: bellemin@unistra.fr

Anna Roglans – Institut de Química Computacional i Catàlisi (IQCC) and Departament de Química, Facultat de Ciències, Universitat de Girona (UdG), Girona 17003 Catalunya, Spain; orcid.org/0000-0002-7943-5706; Email: anna.roglans@udg.edu

Authors

Jordi Vila – Institut de Química Computacional i Catàlisi (IQCC) and Departament de Química, Facultat de Ciències, Universitat de Girona (UdG), Girona 17003 Catalunya, Spain

Miquel Solà – Institut de Química Computacional i Catàlisi (IQCC) and Departament de Química, Facultat de Ciències, Universitat de Girona (UdG), Girona 17003 Catalunya, Spain; orcid.org/0000-0002-1917-7450

Thierry Achard – Institut de Physique et Chimie des Matériaux de Strasbourg, CNRS-Université de Strasbourg, UMR7504, 67034 Strasbourg, France; orcid.org/0000-0001-8271-8718

Anna Pla-Quintana – Institut de Química Computacional i Catàlisi (IQCC) and Departament de Química, Facultat de Ciències, Universitat de Girona (UdG), Girona 17003 Catalunya, Spain; orcid.org/0000-0003-2545-9048

Complete contact information is available at: <https://pubs.acs.org/10.1021/acscatal.2c05790>

Author Contributions

The manuscript was written through contributions of all authors. All authors have given approval to the final version of the manuscript.

Notes

The authors declare no competing financial interest.

ACKNOWLEDGMENTS

We are grateful for financial support from the Ministerio de Ciencia e Innovación (PID2020-113711GB-I00 MCIN/AEI/10.13039/501100011033), the Generalitat de Catalunya (project 2017-SGR-39 and 2021-SGR-623), and the UdG for an IF predoctoral grant to J.V. We also thank Corinne Bailly and Dr. Lydia Karmazin from the University of Strasbourg and Xavier Fontrodona from the University of Girona for the X-ray structural determinations. This work of the Interdisciplinary Thematic Institute QMat, as part of the ITI 2021 2028 program of the University of Strasbourg, CNRS and Inserm, was supported by IdEx Unistra (ANR 10 IDEX 0002) and by SFRI STRAT'US project (ANR 20 SFRI 0012) under the framework of the French Investments for the Future Program.

Open Access funding provided thanks to the CRUE-CSIC agreement with ACS.

REFERENCES

- (1) (a) Tanaka, K. *Transition-Metal-Mediated Aromatic Ring Construction*, 1st ed.; John Wiley & Sons, Inc.: Hoboken, NJ, USA, 2013. (b) Starý, I. G.; Starý, I. Helically chiral aromatics: the synthesis of helicenes by [2 + 2 + 2] cycloisomerization of π -electron systems. *Acc. Chem. Res.* **2020**, *53*, 144–158.
- (2) (a) Lledó, A.; Pla-Quintana, A.; Roglans, A. Allenes, versatile unsaturated motifs in transition-metal-catalyzed [2+2+2] cycloaddition reactions. *Chem. Soc. Rev.* **2016**, *45*, 2010–2023. (b) Domínguez, G.; Pérez-Castells, J. Alkenes in [2+2+2] cycloadditions. *Chem.—Eur. J.* **2016**, *22*, 6720–6739.
- (3) (a) Benson, R. E.; Lindsey, R. V. Chemistry of allene. I. Cyclopolymerization. Synthesis and chemistry of 1,2,4 and 1,3,5-trimethylenecyclohexane and 1,3,5,7-tetramethylenecyclooctane. *J. Am. Chem. Soc.* **1959**, *81*, 4247–4250. (b) Ma, S.; Lu, P.; Lu, L.; Hou, H.; Wei, J.; He, Q.; Gu, Z.; Jiang, X.; Jin, X. What can a metal catalyst do with allenes? One-step formation of steroid scaffolds from readily available starting materials. *Angew. Chem., Int. Ed.* **2005**, *44*, 5275–5278. (c) Ma, S.; Lu, L. Rh(I)-catalyzed bimolecular cyclization between two different 1,5-bisallenes: a combinatorial one-step approach to heterosteroids and mechanistic implications. *Chem.—Asian J.* **2007**, *2*, 199–204. (d) Lu, P.; Ma, S. Rh-catalyzed triple allene approach to bicycle[4.4.0]decene derivatives and its application for the stepwise synthesis of steroid-like tetracyclic skeletons. *Org. Lett.* **2007**, *9*, 5319–5321.
- (4) Sakashita, K.; Shibata, Y.; Tanaka, K. Rhodium-catalyzed cross-cyclotrimerization and dimerization of allenes with alkynes. *Angew. Chem., Int. Ed.* **2016**, *55*, 6753–6757.
- (5) Arai, S.; Izaki, A.; Amako, Y.; Nakajima, M.; Uchiyama, M.; Nishida, A. Regioselective [2+2+2] cycloaddition reaction using allene-ynes with simple allenes under nickel catalysis. *Adv. Synth. Catal.* **2019**, *361*, 4882–4887.
- (6) (a) Brusoe, A. T.; Alexanian, E. J. Rhodium(I)-catalyzed ene-allene-allene [2+2+2] cycloadditions: stereoselective synthesis of complex trans-fused carbocycles. *Angew. Chem., Int. Ed.* **2011**, *50*, 6596–6600. (b) Brusoe, A. T.; Edwankar, R. V.; Alexanian, E. J. Enantioselective intermolecular [2+2+2] cycloadditions of ene-allenes with allenates. *Org. Lett.* **2012**, *14*, 6096–6099.
- (7) Haraburda, E.; Torres, Ò.; Parella, T.; Solà, M.; Pla-Quintana, A. Stereoselective rhodium-catalyzed [2+2+2] cycloaddition of linear allene-ene/yne-allene substrates: reactivity and theoretical mechanistic studies. *Chem.—Eur. J.* **2014**, *20*, 5034–5045.
- (8) (a) Alcaide, B.; Almendros, P.; Aragoncillo, C. Cyclization reactions of bis(allenes) for the synthesis of polycarbo(hetero)cycles. *Chem. Soc. Rev.* **2014**, *43*, 3106–3135. (b) Chen, G.; Jiang, X.; Fu, C.; Ma, S. The diversified reactivities of 1,5-bisallenes. *Chem. Lett.* **2010**, *39*, 78–81.
- (9) (a) Artigas, A.; Vila, J.; Lledó, A.; Solà, M.; Pla-Quintana, A.; Roglans, A. A Rh-catalyzed cycloisomerization/Diels-Alder cascade reaction of 1,5-bisallene for the synthesis of polycyclic heterocycles. *Org. Lett.* **2019**, *21*, 6608–6613. (b) Artigas, A.; Castanyer, C.; Roig, N.; Lledó, A.; Solà, M.; Pla-Quintana, A.; Roglans, A. Synthesis of fused dihydroazepine derivatives of fullerenes by a Rh-catalyzed cascade process. *Adv. Synth. Catal.* **2021**, *363*, 3835–3844.
- (10) Vila, J.; Vinardell, R.; Solà, M.; Pla-Quintana, A.; Roglans, A. A Rh(I)-catalyzed cascade cyclization of 1,5-bisallenes and alkynes for the formation of *cis*-3,4-arylviny pyrrolidines and cyclopentanes. *Adv. Synth. Catal.* **2022**, *364*, 206–217.
- (11) Noucti, N. N.; Alexanian, E. J. Stereoselective nickel-catalyzed [2+2+2] cycloadditions and alkenylative cyclizations of ene-allenes and alkenes. *Angew. Chem., Int. Ed.* **2013**, *52*, 8424–8427.
- (12) Vila, J.; Solà, M.; Pla-Quintana, A.; Roglans, A. Highly selective synthesis of seven-membered azaspiro compounds by a Rh(I)-catalyzed cycloisomerization/Diels-Alder cascade of 1,5-bisallenes. *J. Org. Chem.* **2022**, *87*, 5279–5286.

- (13) (a) Saino, N.; Kogure, D.; Okamoto, S. Intramolecular cyclotrimerization of triynes catalyzed by N-heterocyclic carbene-CoCl₂/Zn or FeCl₃/Zn. *Org. Lett.* **2005**, *7*, 3065–3067. (b) Geny, A.; Gaudrel, S.; Slowinski, F.; Amatore, M.; Chouraqui, G.; Malacria, M.; Aubert, C.; Gandon, V. A straightforward procedure for the [2+2+2] cycloaddition of enediynes. *Adv. Synth. Catal.* **2009**, *351*, 271–275.
- (14) (a) Hoshimoto, Y.; Ohata, T.; Ohashi, M.; Ogoshi, S. Nickel-catalyzed synthesis of N-aryl-1,2-dihydropyridines by [2+2+2] cycloaddition of imines with alkynes through T-shaped 14-electron aza-nickelacycle key intermediates. *Chem.—Eur. J.* **2014**, *20*, 4105–4110. (b) Zhao, J.-P.; Chan, S.-C.; Ho, C.-Y. Substituted 1,3-cyclohexadiene synthesis by NHC-Nickel(0) catalyzed [2+2+2] cycloaddition of 1,n-enyne. *Tetrahedron* **2015**, *71*, 4426–4431. (c) Xue, F.; Loh, Y. K.; Song, X.; Teo, W. J.; Chua, J. Y. D.; Zhao, J.; Hor, T. S. A. Nickel-catalyzed facile [2+2+2] cyclotrimerization of unactivated internal alkynes to polysubstituted benzenes. *Chem.—Asian J.* **2017**, *12*, 168–173. (d) Sánchez, I. G.; Sámal, M.; Nejedlý, J.; Karras, M.; Klívar, J.; Rybáček, J.; Budesinský, M.; Bednárová, L.; Seidlerová, B.; Stará, I. G.; Starý, I. Oxahelicene NHC ligands in the asymmetric synthesis of nonracemic helixenes. *Chem. Commun.* **2017**, *53*, 4370–4373.
- (15) Thakur, A.; Louie, J. Advances in Nickel-catalyzed cycloaddition reactions to construct carbocycles and heterocycles. *Acc. Chem. Res.* **2015**, *48*, 2354–2365 and references cited therein.
- (16) Roglans, A.; González, I.; Pla-Quintana, A. Rhodium N-heterocyclic carbene complexes as effective catalysts for [2+2+2] cycloaddition reactions. *Synlett* **2009**, *2009*, 2844–2848.
- (17) Fernández, M.; Ferré, M.; Pla-Quintana, A.; Parella, T.; Pleixats, R.; Roglans, A. Rhodium-NHC hybrid silica materials as recyclable catalysts for [2+2+2] cycloaddition reactions of alkynes. *Eur. J. Org. Chem.* **2014**, *2014*, 6242–6251.
- (18) For a recent review see: Lee, J.; Hahm, H.; Kwak, J.; Kim, M. New aspects of recently developed rhodium(N-heterocyclic carbene)-catalyzed organic transformations. *Adv. Synth. Catal.* **2019**, *361*, 1479–1499.
- (19) César, V.; Gade, L. H.; Bellemin-Lapponnaz, S. NHC-Cobalt, -Rhodium, and -Iridium Complexes in Catalysis. In *N-Heterocyclic Carbenes*, 2nd ed.; Diez-Gonzales, S., Ed.; RSC Catalysis Series, 2017; pp 302–335.
- (20) (a) Kühn, O. The chemistry of functionalised N-heterocyclic carbenes. *Chem. Soc. Rev.* **2007**, *36*, 592–607. (b) Zhang, W.-H.; Chien, S. W.; Hor, T. S. A. Recent advances in metal catalysts with hybrid ligands. *Coord. Chem. Rev.* **2011**, *255*, 1991–2024. (c) Hameury, S.; de Frémont, P.; Braunstein, P. Metal complexes with oxygen-functionalized NHC ligands: synthesis and applications. *Chem. Soc. Rev.* **2017**, *46*, 632–733. (d) Peris, E. Smart N-heterocyclic carbene ligands in catalysis. *Chem. Rev.* **2018**, *118*, 9988–10031. (e) Neshat, A.; Mastroianni, P.; Mobarakeh, A. M. Recent advances in catalysis involving bidentate N-heterocyclic carbene ligands. *Molecules* **2022**, *27*, 95.
- (21) Fliedel, C.; Braunstein, P. Recent advances in S-functionalized N-heterocyclic carbene ligands: From the synthesis of azolium salts and metal complexes to applications. *J. Organomet. Chem.* **2014**, *751*, 286–300.
- (22) (a) Huynh, H. V.; Yeo, C. H.; Tan, G. K. Hemilabile behavior of a thioether-functionalized N-heterocyclic carbene ligand. *Chem. Commun.* **2006**, 3833–3835. (b) Fliedel, C.; Schnee, G.; Braunstein, P. Versatile coordination modes of novel hemilabile S-NHC ligands. *Dalton Trans.* **2009**, 2474–2476. (c) Huynh, H. V.; Yeo, C. H.; Chew, Y. X. Syntheses, structures, and catalytic activities of hemilabile thioether-functionalized NHC complexes. *Organometallics* **2010**, *29*, 1479–1486. (d) Egly, J.; Bouché, M.; Chen, W.; Maise-François, A.; Achard, T.; Bellemin-Lapponnaz, S. Synthesis, structural characterization and anti-proliferative activity of (κ^1 -C)- and (κ^2 -C,S)-Pt^{II} complexes bearing thioether-functionalized N-heterocyclic carbenes. *Eur. J. Inorg. Chem.* **2018**, *2018*, 159–166. (e) Ulm, F.; Poblador-Bahamonde, A. I.; Choppin, S.; Bellemin-Lapponnaz, S.; Chetcuti, M. J.; Achard, T.; Ritleng, V. Synthesis, characterization, and catalytic application in aldehyde hydrosilylation of half-sandwich nickel complexes bearing (κ^1 -C)- and hemilabile (κ^2 -C,S)-thioether-functionalized NHC ligands. *Dalton Trans.* **2018**, *47*, 17134–17145. (f) De Marco, R.; Dal Grande, M.; Baron, M.; Orjan, L.; Graiff, C.; Achard, T.; Bellemin-Lapponnaz, S.; Pöthig, A.; Tubaro, C. Synthesis, structural characterization and antiproliferative activity of Gold(I) and Gold(III) complexes bearing thioether-functionalized N-heterocyclic carbenes. *Eur. J. Inorg. Chem.* **2021**, *2021*, 4196–4206.
- (23) Wolf, J.; Labande, A.; Daran, J. C.; Poli, R. Nickel(II), Palladium(II) and Rhodium(I) complexes of new NHC-thioether ligands: efficient ketone hydrosilylation catalysis by a cationic Rh complex. *Eur. J. Inorg. Chem.* **2007**, *2007*, S069–S079.
- (24) Sharma, K. N.; Satrawala, N.; Joshi, R. K. Thioether–NHC-ligated Pd^{II} complex for crafting a filtration-free magnetically retrievable catalyst for Suzuki–Miyaura coupling in water. *Eur. J. Inorg. Chem.* **2018**, *2018*, 1743–1751.
- (25) Gandolfi, C.; Heckenroth, M.; Neels, A.; Laurency, G.; Albrecht, M. Chelating NHC Ruthenium(II) complexes as robust homogeneous hydrogenation catalysts. *Organometallics* **2009**, *28*, 5112–5121.
- (26) Szadkowska, A.; Zaorska, E.; Staszko, S.; Pawlowski, R.; Trzybiński, D.; Woźniak, K. Synthesis, structural characterization and catalytic activities of sulfur-functionalized NHC–copper(I) complexes. *Eur. J. Org. Chem.* **2017**, *2017*, 4074–4084.
- (27) Chen, W. G.; Egly, J.; Poblador-Bahamonde, A. I.; Maise-François, A.; Bellemin-Lapponnaz, S.; Achard, T. Synthesis, characterization, catalytic and biological application of half-sandwich ruthenium complexes bearing hemilabile (κ^2 -C,S)-thioether-functionalised NHC ligands. *Dalton Trans.* **2020**, *49*, 3243–3252.
- (28) Egly, J.; Chen, W. H.; Maise-François, A.; Bellemin-Lapponnaz, S.; Achard, T. Half-sandwich ruthenium complexes bearing hemilabile κ^2 -(C,S)-thioether-functionalized NHC ligands: application to amide synthesis from alcohol and amine. *Eur. J. Inorg. Chem.* **2022**, *2022*, No. e202101033.
- (29) Ros, A.; Alcarazo, M.; Monge, D.; Álvarez, E.; Fernández, R.; Lassaletta, J. M. Stereoselective synthesis of cationic heterobidentate C(NHC)/SR rhodium(I) complexes using stereodirecting N,N-dialkylamino groups. *Tetrahedron: Asymmetry* **2010**, *21*, 1557–1562.
- (30) CCDC-2209948, CCDC-2213801, and CCDC-2232591 contain the supplementary crystallographic data for this paper. These data can be obtained free of charge from The Cambridge Crystallographic Data Centre via www.ccdc.cam.ac.uk/data_request/cif.
- (31) César, V.; Bellemin-Lapponnaz, S.; Wadepohl, H.; Gade, L. H. Designing the “search pathway” in the development of a new class of highly efficient stereoselective hydrosilylation catalysts. *Chem.—Eur. J.* **2005**, *11*, 2862–2873.
- (32) The ¹H NMR spectra showed sharp resonances at room temperature and the splitting observed as two multiplets for both CH₂–N and CH₂–S protons at 5.00 and 4.11 and 3.44 and 2.69 ppm respectively is only due to the lack of an effective plane of symmetry in the molecules due to the impeded rotation already observed for NHC-Rh complexes. For similar behaviour see: Jiménez, M. V.; Pérez-Torrente, J. J.; Bartolomé, M. I.; Gierz, V.; Lahoz, F. J.; Oro, L. A. Rhodium(I) complexes with hemilabile N-heterocyclic carbenes: efficient alkyne hydrosilylation catalysts. *Organometallics* **2008**, *27*, 224–234.
- (33) (a) Peñafiel, I.; Pastor, I. M.; Yus, M.; Esteruelas, M. A.; Oliván, M. Preparation, hydrogen bonds, and catalytic activity in metal-promoted addition of arylboronic acids to enones of a rhodium complex containing an NHC ligand with an alcohol function. *Organometallics* **2012**, *31*, 6154–6161. (b) Yu, X. Y.; Patrick, B. O.; James, B. R. New Rhodium(I) carbene complexes from carbene transfer reactions. *Organometallics* **2006**, *25*, 2359–2363. (c) Warsink, S.; Venter, J. A.; Roodt, A. NHC-amide donor ligands in rhodium complexes: Syntheses and characterisation. *J. Organomet. Chem.* **2015**, *775*, 195–201.
- (34) For sulfonamide cases, **3a–3k**, diastereoisomeric ratios were calculated from the reaction crude by NMR spectroscopy. After purification by column chromatography, the corresponding *cis*

diastereoisomer was partially eluted with the cyclotrimerized [2 + 2 + 2] adduct of the acetylene dicarboxylate **2**, making it difficult to measure the diastereoisomeric ratio accurately.

(35) As an experimental evidence of ligand hemilability, bromide abstraction on the neutral Rh complex **RhL4** generated a cationic square planar complex with NHC acting as a bidentate ligand, as deduced from X-ray diffraction experiments (CCDC-2232591) (see [Supporting Information](#) for details).

(36) Seeman, J. I. Effect of conformational change on reactivity in organic chemistry. Evaluations, applications, and extensions of Curtin-Hammett Winstein-Holness kinetics. *Chem. Rev.* **1983**, *83*, 83–134.

(37) Dachs, A.; Osuna, S.; Roglans, A.; Solà, M. A Density functional study of the [2+2+2] cyclotrimerization of acetylene catalyzed by the Wilkinson's catalyst, RhCl(PPh₃)₃. *Organometallics* **2010**, *29*, 562–569.

(38) (a) Inglesby, P. A.; Bacsa, J.; Negru, D. E.; Evans, P. A. The isolation and characterization of a rhodacycle intermediate implicated in metal-catalyzed reactions of alkylidenecyclopropanes. *Angew. Chem., Int. Ed.* **2014**, *53*, 3952–3956. (b) Teng, Q.; Mao, W.; Chen, D.; Wang, Z.; Tung, C.-H.; Xu, Z. Asymmetric synthesis of a fused tricyclic hydronaphthofuran scaffold by desymmetric [2+2+2] cycloaddition. *Angew. Chem., Int. Ed.* **2020**, *59*, 2220–2224. (c) Hong, X.; Stevens, M. C.; Liu, P.; Wender, P. A.; Houk, K. N. Reactivity and chemoselectivity of allenes in Rh(I)-catalyzed intermolecular (5 + 2) cycloadditions with vinylcyclopropanes: allene-mediated rhodacycle formation can poison Rh(I)-catalyzed cycloadditions. *J. Am. Chem. Soc.* **2014**, *136*, 17273–17283. (d) Casitas, A.; Krause, H.; Lutz, S.; Goddard, R.; Bill, E.; Fürstner, A. Ligand exchange on and allylic C-H activation by iron(0) fragments: π -complexes, allyliron species, and metallacycles. *Organometallics* **2018**, *37*, 729–739. (e) Schobert, R. Chelated η^2 -alkene- and η^3 -allyl-carbene complexes of late transition metals: structure-reactivity relations and preparative use. Part 10. The chemistry of metallacyclic alkenylcarbene complexes. *J. Organomet. Chem.* **2001**, *617–618*, 346–359.

(39) Schore, N. E. Transition-metal-mediated cycloaddition reactions of alkynes in organic synthesis. *Chem. Rev.* **1988**, *88*, 1081–1119.

(40) Roglans, A.; Pla-Quintana, A.; Solà, M. Mechanistic studies of transition-metal-catalyzed [2 + 2 + 2] cycloaddition reactions. *Chem. Rev.* **2021**, *121*, 1894–1979.

(41) (a) Kozuch, S.; Shaik, S. Kinetic-quantum chemical model for catalytic cycles: the Haber–Bosch process and the effect of reagent concentration. *J. Phys. Chem. A* **2008**, *112*, 6032–6041. (b) Kozuch, S.; Shaik, S. How to conceptualize catalytic cycles? The energetic span model. *Acc. Chem. Res.* **2011**, *44*, 101–110.